Oil & Gas Science and Technology - Rev. IFP Energies nouvelles **73**, 19 (2018)

https://doi.org/10.2516/ogst/2018015

Available online at:
www.ogst.ifpenergiesnouvelles.fr

REGULAR ARTICLE

OPEN ACCESS

Kinetics study and simulation of CO_2 absorption into mixed aqueous solutions of methyldiethanolamine and hexylamine

Ammar Mehassouel[1,*], Ratiba Derriche[1], and Chakib Bouallou[2]

[1] Ecole Nationale Polytechnique, Laboratoire de valorisation des énergies fossiles, El Harrach, Algerie
[2] MINES ParisTech, PSL Research University, CES -Centre d'efficacité énergétique des systèmes- 60, Boulevard Saint Michel, Paris, France

Received: 27 October 2017 / Accepted: 23 April 2018

Abstract. This study investigated kinetics of CO_2 absorption into mixed methyldiethanolamine (MDEA) and hexylamine (HA) solutions in a Lewis cell reactor. The experiments were conducted in the temperatures 298, 313 and 333 K with mass concentrations MDEA 37 wt.% + HA 3 wt.%, MDEA 35 wt.% + HA 5 wt.% and MDEA 33 wt.% + HA 7 wt.%. Our results showed that adding a small amount of hexylamine enhances the kinetics of CO_2 absorption and that the kinetics of CO_2 absorption with aqueous MDEA 37 wt.% + HA 3 wt.% is pseudo first order regime with reduced activation energy compared to that of MDEA 40 wt.%. The absorption/regeneration system was simulated using Aspen plus^{TM} software for the treatment of gas streams from cement plant in a post-combustion process. The analysis of our results established that blended solvent MDEA 37 wt.% + HA 3 wt.% gives lower energy consumption than that of MDEA 40 wt.%.

1 Introduction

Human activities have gradually increased the atmospheric concentration of greenhouse gases such as CO_2, methane, nitrous oxide and chlorofluorocarbons over the past century. According to the 5th report of the Intergovernmental Panel on Climate Change (IPCC, 2013), the Earth will continue to warm up as a result of human activities; the temperature will rise by 0.3–4.8 °C. There are various methods for capturing CO_2 (Kanniche *et al.*, 2010) such as, the chemical absorption method which is the most used for CO_2 capture using a usually amine-based chemical solvent. There are different types of amines:

- the primary amines such as monoethanolamine (MEA) and diglycolamine (DGA), which are characterized by their very large reactivity and low absorption capacity;
- secondary amines such as diethanolamine (DEA) and diisopropylamine (DIPA), which are less reactive than the primary amines; the reaction of these amines (primary and secondary) with CO_2 forms a carbamate;
- tertiary amines such as N-methyldiethanolamine (MDEA) and triethanolamine (TEA) which are characterized by their low reactivity and a high absorption rate.

For MDEA, one mole of amine is required to absorb one mole of CO_2, besides, it is very resistant to thermal and chemical degradation, the reaction of tertiary amines with CO_2 does not form a carbamate. Therefore, the energy required for the regeneration of these amines is low, which allows to minimize the cost of the capture process. Several studies have shown that the mixture of primary and tertiary amines combines the high absorption capacity of tertiary amines with the high reactivity of primary and secondary amines (Paul *et al.*, 2009; Zoghi *et al.*, 2012; Toro-Molina and Bouallou, 2013). The regeneration costs of mixtures can be reduced compared to those of MEA or DEA. Thus, the use of amine mixtures can improve the efficiency of gas treatment processes. However, these processes always require lots of energy during desorption. Therefore, the key problems are, how to reduce the energy penalty, and how to reduce the capture cost. Recently the demixing solvents (DMX^{TM}) have been developed by the IFP Energies nouvelles to reduce the operating cost by phase splitting in decanter before steam stripping (Lecomte *et al.*, 2009; Aleixo *et al.*, 2011; Raynal *et al.*, 2011a, b; Xu *et al.*, 2012). The process consists of using aqueous amine solutions that are capable to form two immiscible liquid phases at a given temperature and concentration in CO_2.

The principle of these demixing solvents is to absorb the carbon dioxide in the aqueous solution of demixing amine. A monophasic solution loaded with CO_2 is then obtained. After heating, the formation of two distinct phases is

* Corresponding author: ammar.mehassouel@g.enp.edu.dz

observed, one poor in CO_2 and rich in amine, the other rich in CO_2 and poor in amine, the phase that is poor in CO_2 can directly be recycled to absorber. Demixation can be controlled by temperature, it occurs above a given temperature value (lower critical solution temperature), above which the two phases are not miscible. The other amines that have emerged in recent years are lipophilic amines, hybrid molecules with hydrophilic and hydrophobic functional groups; they form two phases during regeneration. The organic phase acts as an extractive agent (Tan, 2010), this characteristic allows capturing CO_2 at a low cost. Several amines with phase change have been studied. Zhang *et al.* (2011) studied the absorption of CO_2 by a mixture of DMCA + DPA and found a precipitation of DPA at high CO_2 loading, they found that this mixture is more efficient than the monoethanolamine (MEA 30 wt. %), because it allows to minimize the regeneration temperature of 120 °C for MEA 30 wt.% at a temperature below 80 °C, which allows to minimize the energy required for regeneration. Zhang *et al.*(2012a, b) investigated different lipophilic amines for improving the energy efficiency of post combustion, they classified them into two categories: activators as hexylamine (HA) and dipropylamine (DPA) and regeneration promoters such as N-ethylpiperidine (EPD), N,N-dimethylcyclohexylamine (DMCA), N-methylpiperidine (MPD) and dibutylamine (DBA). The decrease of the aqueous amine solubility while the temperature increases causes phase separation above the Lower Critical Solution Temperature (LCST). Zhang *et al.* (2013) studied the mixture of methylcyclohexylamine (MCA) and dimethylcyclohexylamine and 2-amino 2-methyl propylamine (AMP) as solubilizer, the addition of AMP increases the solvent efficiency as well as LCST. The percentage of the solubilizer should not exceed 15 wt.%.

Xu *et al.* (2013) investigated several lipophilic amines alone and mixed with different concentrations in order to select the best lipophilic solvent. Ye *et al.* (2015) studied several mixtures of lipophilic amines as activators for dimethylcyclohexylamine (DMCA) on one hand and with diethylethanolamine (DEEA) on the other hand.

Wang *et al.* (2017) investigated the kinetics of CO_2 absorption with the solvent N,N-diethylethanol amine (DEEA) and N,N-dimethylbutylamine (DMBA), the mixture forms two phase during absorption; it has a high absorption rate and low energy consumption compared to the conventional MEA solvent. Ye *et al.* (2017) studied the mechanism of absorption and desorption of CO_2 with phase transitional diethylene triamine (DETA) and pentamethyl diethylenetriamine (PMDETA). Knuutila and Nannestad (2017) studied the effect of the concentration of 3-(methylamino)-propylamine (MAPA) on the heat of CO_2 absorption in DEEA/MAPA blend.

Mehassouel *et al.* (2016) used the hexylamine (lipophilic amine) to activate methyldiethanolamine (MDEA). Pinto *et al.* (2013) studied the CO_2 absorption with blend 5M (DEEA) and 2M of 3-(methylamino)-propylamine (MAPA).

In parallel in recent years studies have also focused on reducing the concentration of CO_2, its conversion and its use for the production of high value products. Among these works, Tursunov *et al.* (2017) studied the conversion of CO_2 to methanol by hydrogenation using over copper and iron based catalysts as well as the influence of the different parameters on the conversion rate and the reaction mechanism. Bashipour *et al.* (2017) investigated the production of sodium sulphate (Na_2S) by the absorption of H_2S in NaOH in a spraying column. Na_2S has several applications in the chemical industry, the authors have used the Response Surface Methodology (RSM) to design and optimize experiments based on Central Composite Design (CCD). A model of Artificial Neural Network has also been used to predict the percentage by weight of Na_2S. Passalacqua *et al.* (2015) studied the possibility of converting CO_2 into fuel in the presence of solar energy and water in a direct photoreactor, the product obtained is a mixture of methane, methanol and formic acid.

Concerning the simulation part, Sharifi and Omidbakhsh (2017) simulated the capture of CO_2 by solvent MDEA using different types of absorption and regeneration columns, to select the best type in terms of absorption capacity. The cement industry is one of the most emitting industries of CO_2. It represents about 5% of the total emissions. Cement plant flue gas has a relatively high CO_2 concentration, typically about 25 mol% compared to about 14 mol% for a coal fired power plant (IEA, 2008) the emission of CO_2 comes from fossil fuel combustion in the kiln process and de-carbonation of limestone ($CaCO_3$) to Calcium Oxide (CaO) (Bosoaga *et al.*, 2009). Among the authors who studied the simulation to capture CO_2 coming from a cement plant; Nazmul (2005) used the solvent MEA (30 wt%).

The aim of our work is to study the kinetics of CO_2 absorption by a mixture of methyldiethanolamine (MDEA) activated by hexylamine in different concentrations, the selected solvent is used to simulate the CO_2 capture coming from a cement plant.

2 Experimental

2.1 Chemicals

All the solutions have been prepared with deionized water. MDEA was obtained from *Sigma Aldrich* with 98% mass purity, HA was obtained from *Acros Organics* with 98% mass purity, CO_2 was provided by *Air Liquid* with a certified purity of 99.99 vol%.

2.2 Density and viscosity measurement

The density and viscosity of all the solutions prepared MDEA 33 wt.% + HA 7 wt.%, MDEA 35 wt.% + HA 5 wt. %, MDEA 37 wt.% + HA 3 wt.% and MDEA 40 wt.%, were measured by a Anton Paar densimeter in different temperatures 298 K, 313 K and 333 K (Tab. 1).

2.3 Liquid side mass transfer coefficient

The value of physical mass transfer coefficient (k_L) of CO_2 in aqueous solutions was obtained from mass transfer correlation between dimensionless numbers Reynolds (Re), Schmidt (Sc) and Sherwood (Sh). This correlation (Eq. 1)

Table 1. Density and viscosity measurement for different solvents.

T (K)	C_{HA} (wt.%)	C_{MDEA} (wt.%)	ρ (g cm^{-3})	μ (Pa s)·10^3
298	0	40	1.0295	4.797367
	3	37	1.0225	5.042459
	5	35	1.0149	4.838942
	7	33	1.0116	5.044242
313	0	40	1.0209	2.905992
	3	37	1.0137	2.999944
	5	35	1.0059	2.914595
	7	33	1.0028	3.028657
333	0	40	1.0085	1.734015
	3	37	1.0000	1.727800
	5	35	0.9931	1.719255
	7	33	0.9895	1.756758

has been obtained by Amrarene and Bouallou (2004) based on measurements of physical absorption of N_2O in aqueous solutions of MDEA.

$$\mathrm{Sh} = 0.352 \times \mathrm{Re}^{0.618} \times \mathrm{Sc}^{0.434}, \quad (1)$$

$$\mathrm{Re} = \frac{\rho N d_{Ag}^2}{\mu}, \quad (2)$$

$$\mathrm{Sc} = \frac{\mu}{\rho D_i}, \quad (3)$$

$$\mathrm{Sh} = \frac{k_L d_{cell}}{D_i}. \quad (4)$$

This correlation is valid for:

$$215 < \mathrm{Re} < 5666,$$

$$46 < \mathrm{Sc} < 21710,$$

$$378 < \mathrm{Sh} < 985,$$

μ = dynamic viscosity (Pa s), d_{cell} = inner diameter of the Lewis cell (m), D = diffusivity (m^2 s^{-1}), d_{Ag} = diameter of the Rushton turbine (m), ρ = solution density (kg m^{-3}). The validity of this correlation has been tested for our experiments in different temperatures and for different solvents studied (see Appendix B).

The diffusion coefficient and the Henry constant are obtained by applying the correlation of Al-Ghawas *et al.* (1989), for MDEA compositions up to 50 wt.%. The influence of the hexylamine concentration is considered negligible. The equations used are given in Appendix A, N = 100 rpm is the stirring speed of the liquid phase; it is maintained constant during the experiment.

2.4 Experimental setup and procedure

2.4.1 Experimental apparatus

The apparatus used for carrying out the kinetic measurements (Fig. 1) (Toro-Molina and Bouallou, 2013), is a double jacket cell reactor whose temperature is kept constant by means of a control bath. The cell is made of Pyrex glass of 63.3×10^{-3} m internal diameter, whose two extremities are sealed up by two metal flanges, joints ensuring the seal of the assembly. Four Teflon counter-blades are placed inside the cell, in order to avoid the formation of a vortex and also to maintain a stable horizontal ring. This ring allows to stabilize and to define a gas-liquid interfacial area that is equal to 15.34×10^{-4} m^2. The value of k_L remains constant in the various solutions tested. The liquid phase agitator is assured by Rushton turbine with six-bladed 42.5×10^{-3} m in diameter; the gas phase is stirred by four-bladed impeller 40×10^{-3} m in diameter. The agitators of the liquid and gas phase are driven by a variable speed motor. The upper flange is connected to a Druck pressure sensor thermostatically controlled to 373 K in order to avoid any phenomenon of condensation in its support which permits to measure pressures up to 2.5×10^5 Pa. The lower flange is equipped with a temperature sensor and a non-rotating needle valve. The temperature sensor and the pressure sensor are connected to an absorption data acquisition unit.

2.4.2 Procedure

The aqueous solutions were prepared under vacuum, the water and the amine were mixed by gravity according to the concentration of the required aqueous solution, and the mass of water and amine were measured by weight. The cell must be evacuated before introducing the solvent into the reactor when the working temperature and pressure are stabilized in the cell. The volume of the liquid phase is measured based on the mass of the solution introduced and its density, in this case, the contact between the solvent and the CO_2 is initiated and the acquisition of data begins. The reproducibility of the absorption rate is within 10%.

During the data acquisition, the pressure in the cell is recorded as shown in Figure 2. The pressure within the cell can be divided into four periods:

- solvent vapor pressure at equilibrium;
- injection of the gas into the cell, which results in an increase in pressure;
- absorption of the gas by the solvent;
- return to system balance.

By way of illustration, Figure 3 shows the CO_2 absorption by aqueous MDEA 37 wt.% + HA 3 wt.% solvent at 298 K.

2.4.3 Results and discussion

The absorption measurements were carried out at three different temperatures 298 K, 313 K and 333 K for the three solvents MDEA 37 wt.% + HA 3 wt.%, MDEA 35 wt.% + HA 5 wt.% and MDEA 33 wt.% + HA 7 wt.%.

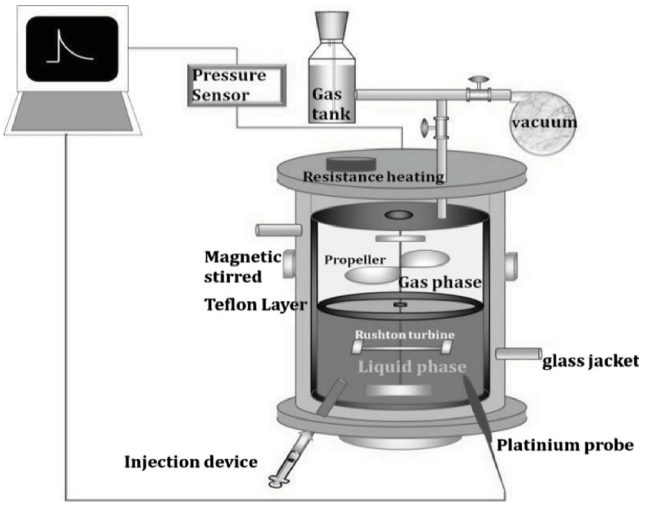

Fig. 1. Experimental apparatus.

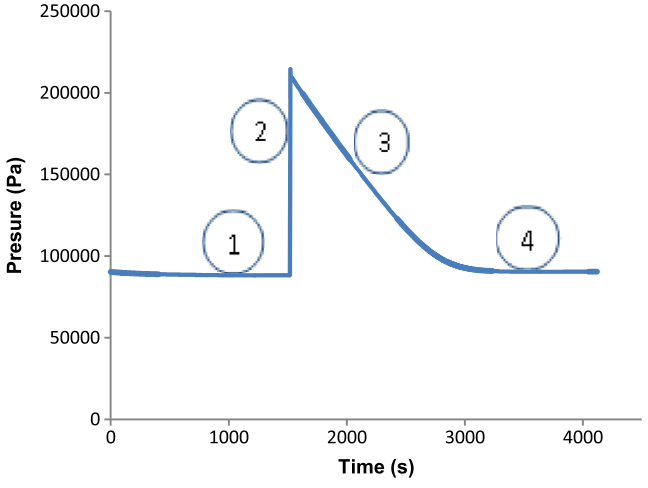

Fig. 2. Data acquisition example for CO_2 absorption in aqueous solution.

A material balance on the CO_2 gas phase of the reactor allows us to directly determine the absorption flux:

$$\phi_{CO_2} \cdot a = \frac{d(n_{CO_2})}{dt} = -\frac{V_g}{RT} \cdot \frac{d(P_{CO_2})}{dt}. \quad (5)$$

a is the interfacial area and V_g is the volume of gas.

The influence of the kinetics of the chemical reaction on the CO_2 absorption is reflected by the enhancement factor E, in this case, the absorption flux (Eq. 5) is written assuming that the concentration of CO_2 in the liquid phase is very small compared to its concentration at the interface:

$$\phi_{CO_2} = E \cdot k_L C_{CO_2 int}. \quad (6)$$

The gas phase is assumed ideal and the concentration of CO_{2int} at the interface is connected with its pressure via the Henry law:

$$P_{CO_2} = H_{CO_2} \cdot C_{CO_2 int}. \quad (7)$$

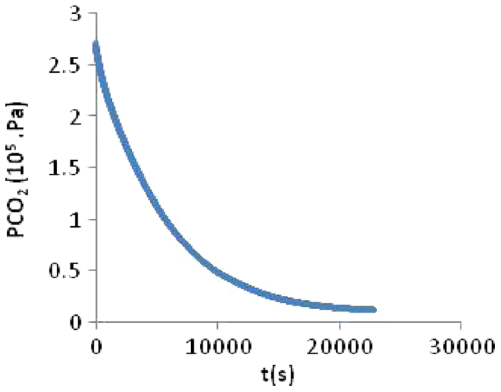

Fig. 3. CO_2 absorption by aqueous MDEA 37 wt.% + HA 3 wt.% solvent at 298 K.

P_{CO_2} is the pressure of CO_2:

$$P_{CO_2} = P - P_{sol}, \quad (8)$$

where P is the total pressure in the cell and P_{sol} is the vapor pressure in the cell before introducing the solvent.

The initial absorption rates are measured within a pressure range of 10 kPa from the initial total pressure, for this small pressure drop, the concentration of CO_2 resulting from the absorption does not change much the composition of the solution so, k_L, HCO_2, and E remains constant with time. The integration of Equation (5) using Equations (6)–(8) give:

$$\mathrm{Ln}\left(\frac{P - P_{sol}}{P_0 - P_{sol}}\right) = -\beta \cdot t, \quad (9)$$

$$\beta = \frac{\mathrm{RT}}{V_G \cdot H_{CO_2}} \cdot k_L \cdot E \cdot a, \quad (10)$$

β is the slop (s^{-1}), the enhancement factor E is obtained from β using Equation (10).

The condition of the pseudo first order reaction regime between CO_2 and blend MDEA + HA is tested, in this case, we have:

$$r_{ov} = r_{CO_2-HA} + r_{CO_2-MDEA}, \quad (11)$$

$$r_{ov} = k_{CO_2-HA} C_{CO_2} C_{HA} + k_{CO_2-MDEA} C_{CO_2} C_{MDEA}, \quad (12)$$

$$r_{ov} = k_{ov} C_{CO_2}, \quad (13)$$

$$E = \mathrm{Ha} = \frac{\sqrt{k_{ov}} D_{CO_2}}{K_l}, \quad (14)$$

$3 < \mathrm{Ha} < E_i/2$, k_{ov} is the overall reaction rate constant, it is calculated using Equation (14), and Ha is the Hatta number that allows us to locate the place of the reaction:

- $\mathrm{Ha} < 0.3$: in the liquid phase.
- $0.3 < \mathrm{Ha} < 3$: both in the liquid phase and in the film diffusion.
- $\mathrm{Ha} > 3$ in the film diffusion.

Table 2. Different parameters results for CO_2 absorption.

Solvent (wt.%)	T (K)	$V_G{\cdot}10^6$ (m^3)	$b{\cdot}10^3$ (s^{-1})	$D_{amine}{\cdot}10^9$ ($m^2\,s^{-1}$)	$D_{CO2}{\cdot}10^9$ ($m^2{\cdot}s^{-1}$)	H_{CO2} $Pa\,m^3\,mol^{-1}$	$k_L{\cdot}10^{-5}$ ($m\,s^{-1}$)	E	E_i
MDEA40	298	196.24	0.4	0.148	0.50	3663.72	0.772	9.80	19.81
MDEA37 + HA3	298	192.27	0.3	0.14	0.48	3670.58	0.74	7.46	14.20
	313	184.01	0.6	0.24	0.80	4625.24	1.12	11.38	26.20
	333	188.69	0.78	0.46	1.45	6024.47	1.77	11.76	25.13
MDEA35 + HA5	298	208.41	9.0	0.14	0.5	3677.41	0.76	236.92	25.11
	313	207.55	9.5	0.25	0.82	4629.39	1.14	200.32	32.31
	333	203.92	9.2	0.46	1.45	6020.08	1.78	148.87	19.87
MDEA33 + HA7	298	185.48	5.9	0.14	0.48	3578.97	0.74	138.31	22.18
	313	197.85	5.42	0.24	0.8	4633.51	1.25	99.56	17.52
	333	184.72	4.6	0.46	1.46	5884.63	1.19	66.03	23.11

The film theory suppose that the resistance of mass transfer is located in a thin film adjacent to the gas-liquid interface, the mass transfer on the liquid phase is carried out only by molecular diffusion (Whitman, 1923).

E_i is the instantaneous enhancement factor which is also determined according to Equation (15):

$$E_i = 1 + \frac{D_{\text{reactif}} {}^{*} C_{\text{reactif}}}{D_{CO_2} {}^{*} C_{CO_2}}. \tag{15}$$

Table 2 summarized the different parameters results for CO_2 absorption by different amine mixtures at different temperatures.

The results show that the reaction takes place in the film diffusion, the Hatta numbers are all greater than 3. The condition of pseudo first order reaction is satisfied for the mixture MDEA 40 wt.% at 298 K, and the mixture MDEA 37 wt.% + HA 3 wt.% at 298 K, 313 K and 333 K.

The condition of pseudo first order reaction is not satisfied for the mixtures MDEA 35 wt.% + HA 5 wt.% and MDEA 33 wt.% + HA 7 wt.%. This may be due to several factors: firstly, the mixtures form two phases in the working temperature range, because, hexylamine which is lipophilic amine, has very low aqueous solubility, and the miscibility changes with temperature and mass concentration of amine, phenomenon that is already studied by Bishnoi and Rochelle (2002) for the absorption of CO_2 by the mixture of MDEA + PZ, the piperazine which has a low aqueous solubility can give two phases. Secondly, the presence of hexylamine can lead to errors in the calculation of the physical properties of the solutions.

We can also note that the addition of a small amount of hexylamine substantially increases the kinetics of CO_2 absorption for a given temperature (Figs. 4 and 5), this is due to hexylamine which has very fast absorption (Tan, 2010), and high capacity, so, the CO_2 reacts firstly with hexylamine in the blend MDEA + HA, the CO_2 loading increases within a short time of absorption. The increase in the hexylamine concentration decreases the fraction of MDEA, result in a decrease in CO_2 loading capacity for aqueous MDEA 35 wt.% + HA 5 wt.% and MDEA 33 wt.% + HA 7 wt.%. The aqueous solubility decreases as the temperature increases causing phase separation, thus a decrease in the CO_2 loading capacity for the MDEA 37 wt.% + HA 3 wt.% solvent at 333 K (Fig. 5).

The calculation of the activation energy for the reaction of CO_2 with aqueous mixture MDEA 37 wt.% + HA 3 wt.% (Fig. 6) is carried out by applying the Arrhenius law.

$$\ln(k_{CO_2-\text{MDEA 37 wt.\% + HA 3 wt.\%}}) = \ln(A) - \frac{\text{Ea}}{\text{RT}}, \tag{16}$$

where $k_{CO_2-\text{MDEA 37 wt.\% + HA 3 wt.\%}}$ is the second order kinetics constant for the reaction of CO_2 with blend MDEA 37 wt.% + HA 3 wt.%.

The calculated activation energy (Ea) is 22. 25 Kj mol^{-1}, which is very small compared to MDEA 40 wt.% that is equal to 44.3 KJ · mol^{-1} (Amann and Bouallou, 2009; Cadours and Bouallou, 1998). The overall rate law is:

$$k_{CO_2-\text{MDEA 37 wt.\% + HA 3 wt.\%}} = 26.78{*}10^2{*}\exp\left(\frac{-2678.5}{T}\right)_{(m^3\cdot s^{-1}\cdot mol^{-1})}. \tag{17}$$

The diminution in the activation energy for the reaction of CO_2 with aqueous solution of MDEA 37 wt.% + HA 3 wt.% decreases the energy demand for solvent regeneration.

The mixture MDEA 37 wt.% + HA 3 wt.% has very fast absorption rate and high capacity compared with MDEA 40 wt.% and compared to other solvents MDEA 35 wt.% + HA 5 wt.% and MDEA 33 wt.% + HA 7 wt.% at 298 K (Fig. 7). The explanations for this behavior can be either, the stability of the hexylamine carbamate for the reaction of CO_2 with aqueous solution MDEA 37 wt.% + HA 3 wt.% is very low or, there is any formation of the carbamate in the solution, resulting into a high amount of free amine in the solution available to react with CO_2.

We can also say that, the absorption which is an exothermic phenomenon is favored at temperature 298 K.

3 Simulation

The Aspen Plus^{TM} software was used to simulate the capture of CO_2 by aqueous MDEA with two different mass concentrations (MDEA 40 wt.% and MDEA 50 wt.%) and

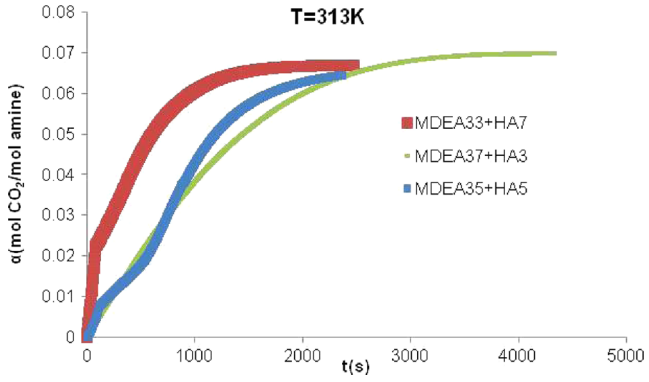

Fig. 4. CO_2 loaded *versus* time for different solvents at 313 K.

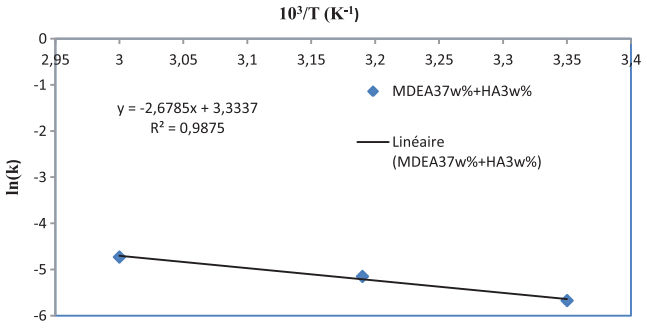

Fig. 6. Arrhenius law for the CO_2 absorption in aqueous MDEA 37 wt.% + HA 3 wt.% solution.

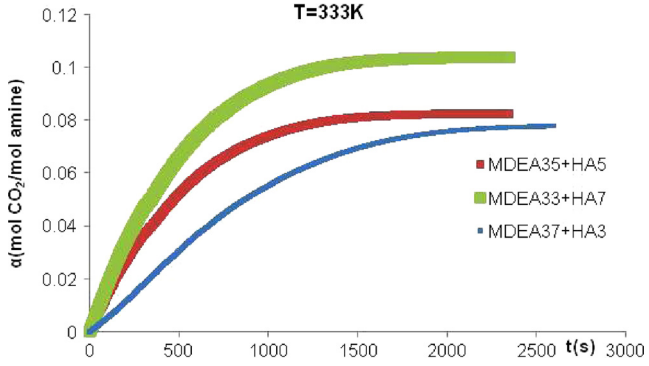

Fig. 5. CO_2 loaded *versus* time for different solvents at 333 K.

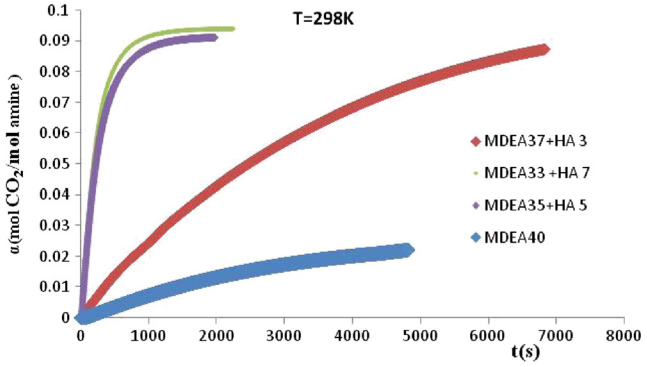

Fig. 7. CO_2 loaded *versus* time for different solvents at 298 K.

Table 3. Composition of the gas stream before introducing to the absorber.

Composition	CO_2	H_2O	N_2	O_2
(% mol)	36.3	2.8	59.5	1.3
Flow rate (kmol/h)	3204.014	249.5783	5248.308	115.4059

with MDEA 37 wt.% + HA 3 wt.%. The flue gas studied was coming from the cement plant, its composition before introducing to the absorber is shown in Table 3. It is in 0.12 MPa and 313 K, Figure 8 shows the alkanolamine process for CO_2 capture. CO_2 is washed by a countercurrent with the solvent. The rich solvent leaving the absorber is pumped by P1 to 0.21 MPa and sent to heat exchange where it is preheated by the regenerated solvent recovered at the bottom of the stripper. After regeneration, the lean solvent is pumped by P2 to 0.21 MPa and cooled at 0.12 MPa and 313 K before recycling to the absorber. The CO_2 stream at the top of the stripper is compressed to 15 MPa in a multi stage compressor.

We have used the ELectrolyte Non-Random Two Liquid activity coefficients (ELECNRTL) thermodynamic model for the CO_2 capture simulation by the Aspen Plus^{TM} software, this model allows simulating non-ideal aqueous solutions, while Aspen Plus^{TM} has the KEMDEA inserts data package for the simulation with the solvent MDEA. For MDEA 37 wt.% + HA 3 wt.%, we modified the insert data package used for the simulation with MDEA (KEMDEA) by adding the CO_2 reactions with hexylamine (Eqs. 18 and 19).

$$HA^+ + \leftrightarrow HA + H_3O^+, \tag{18}$$

$$HACOO^- + H_2O \leftrightarrow HA + HCO_3^-. \tag{19}$$

The parameters of binary interactions between MDEA and hexylamine as well as electrolytic pair interactions and kinetic constants reaction were regressed from experimental data using the Aspen Plus^{TM} Data Regression System (DRS), module which was already used by lot of literature studies (Pinto *et al.*, 2013; Aroua *et al.*, 2002; Mudhasakul *et al.*, 2013).

The study of sensitivity was carried out based on the number of the theoretical stages of the absorber and the stripper. It was conducted in the aim to minimize, the solvent flow rate in the absorber and the heat duty in the reboiler. For 85% CO_2 recovery, Figure 9 shows the evolution of energy regeneration with lean CO_2 loading and concentration for all solvent studied. It is clear that MDEA 50 wt.% gives a lower energy regeneration compared to MDEA 40 wt.%, the low energy for solvent MDEA 40 wt.% is equal to 3.45 GJ/tCO_2, whereas for lean CO_2 loading it is equal to 0.115.

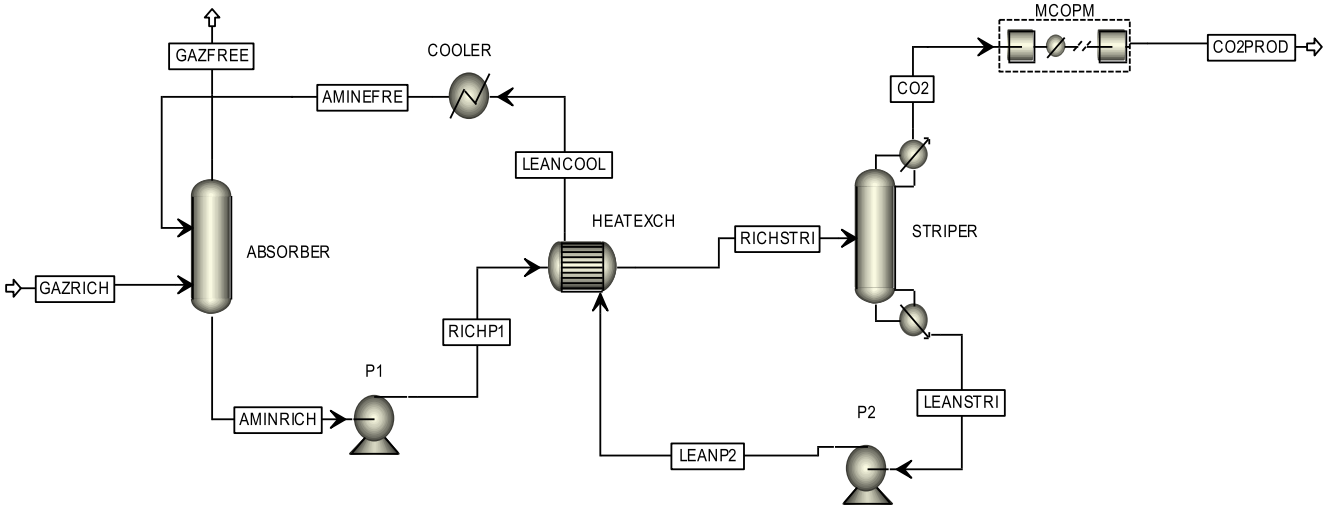

Fig. 8. Alkanolamine process for CO_2 capture.

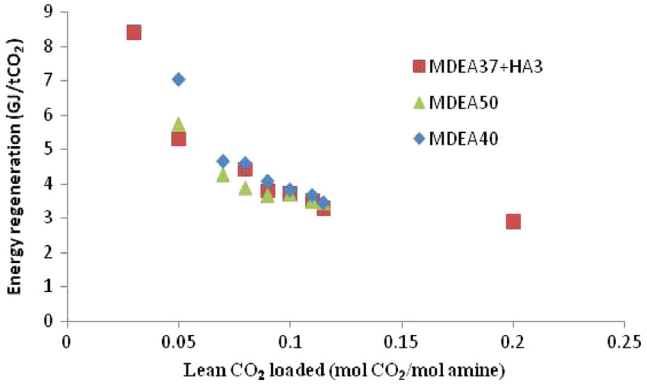

Fig. 9. Energy regeneration for differents lean CO_2 loaded.

For MDEA 37 wt.% + HA 3 wt.% solvent, the low energy is equal to 2.9 GJ/tCO_2 whereas for lean CO_2 loading it is equal to 0.2 (Tab. 4).

4 Conclusion

The aim of this study was to find the most favorable blend composition to capture CO_2. CO_2 absorption rates into MDEA-HA aqueous solutions are measured at three temperatures 298 K, 313 K and 333 K, and different mass concentrations MDEA 37 wt.% + HA 3 wt.%, MDEA 35 wt.% + HA 5 wt.% and MDEA 33 wt.% + HA 7 wt.%. HA is very reactive with CO_2, it was proposed to use this amine as an activator for an aqueous MDEA solution. The addition of HA leads to a significant enhancement of the absorption rates compared to an aqueous MDEA 40 wt.% solution. Results show that kinetics absorption of blended MDEA 37 wt.% + HA 3 wt.% is pseudo first order. Comparative simulations for CO_2 capture of flue gas for a cement plant shows that MDEA 37 wt.% + HA 3 wt.% solvent leads to lower energy consumption than those of MDEA 40 wt.%.

Table 4. Performance of solvents regarding energy consumption of the reboiler (CO_2 recovery = 85%).

Solvent	MDEA 40	MDEA 37 + HA 3
Lean CO_2 loading (mol CO_2/mol solvent)	0.115	0.2
Absorber trays	4	4
Striper trays	4	4
Energy consumption (GJ/tCO_2)	3.45	2.9

Nomenclature

a	interfacial area (m^2)
C_i	concentration of component i ($mol\,m^{-3}$)
DRS	data regression system
d_{ag}	Rushton turbine diameter (m)
d	density of the solution ($kg\,m^{-3}$)
D_i	diffusivity of species i in liquid phase ($m^2\,s^{-1}$)
d_{cel}	internal cell diameter (m)
E	enhancement factor
E_i	instantaneous enhancement factor
Ea	activation energy ($KJ\,mol^{-1}$)
ELECNRTL	electrolyte non-random two liquid activity coefficients
H_{CO2}	Henry's law constant ($Pa\,m^3\,mol^{-1}$)
Ha	Hatta number
IEA	international energy agency
k_L	liquid side mass transfer coefficient ($m\,s^{-1}$)
k_{OV}	overall rate constant (s^{-1})
KEMDEA	insert data package for MDEA
k	equilibrium constant
n	number of mole (mol)
N	stirrer speed (rpm)
P	pressure (Pa)
R	ideal gas constant ($8.314\,J\,K^{-1}\,mol^{-1}$)

Re	Reynolds number
Sc	Schmidt number
Sh	Sherwood number
t	time (s)
T	temperature (K)
V	volume (m^3)
χ_i	mole fraction of component i

Greek symbols

μ	dynamic viscosity (Pa s)
ϕ	chemical absorption rate ($mol\,m^{-2}\,s^{-1}$)
β	slop (s^{-1})

Subscripts and superscripts

Sol	solvent
Int	interface
L	liquid
0	initial

Abbreviations

CO_2	carbon dioxide
$CaCO_3$	limestone
CaO	calcium oxide
DGA	diglycolamine
MDEA	N-methyldiethanolamine
DEA	diethanolamine
DIPA	diisopropylamine
DMCA	dimethylcyclohexylamine
DPA	dipropylamine
DEEA	2-(diethyl amino)-ethanol
DETA	diethylenetriamine
DMBA	N.N.dimethylbutylamine
DMX^{TM}	demixing solvent
EPD	N-ethylpiperidine
HA	hexylamine
LCST	low critical solution temperature
MPD	N-methylpiperidine
MEA	monoethanolamine
MAPA	3-(methylamino)-propylamine
MCA	methylcyclohexylamine
N_2O	nitrous oxide
PZ	piperazine
PMDETA	pentamethyldiethylenetriamine
TEA	triethanolamine

References

Aleixo M., Prigent M., Gibert A., Porcheron F., Mokbel I., Joseb J., Jacquin M. (2011) Physical and chemical properties of DMX^{TM} solvents, *Energy Procedia* **4**, 148–155.

Al-Ghawas H.A., Hagewiesch D., Ruiz-Ibanez G., Sandall O. (1989) Physicochemical properties important for carbon dioxide absorption in aqueous methyldiethanolamine, *J. Chem. Eng. Data.* **34**, 385–391.

Amann J.-M.G., Bouallou C. (2009) Kinetics of the absorption of CO_2 in aqueous solution of N-methyldiethanolamine + triethylenetetramine, *Ind. Eng. Chem. Res.* **48**, 3761–3770.

Amrarene F., Bouallou C. (2004) Kinetics of carbonyl sulfide (COS) absorption withaqueous solution of diethanolamine and methyldiethanolamine, *Ind. Eng. Chem. Res.* **43**, 6136–6141.

Aroua M.K., Haji-Sulaiman M.Z., Ramasamy K. (2002) Modelling of carbon dioxideabsorption in aqueous solutions of AMP and MDEA and their blends using Aspen plus, *Sep. Purif. Technol.* **29**, 153.

Bashipour F., Rahimi A., Nouri Khorasani S., Naderinik A. (2017) Experimental optimization and modeling of sodium sulfide production from H_2S-rich off-gas via response surface methodology and artificial neural network, *Oil Gas Sci. Technol. – Rev. IFP Energies nouvelles* **72**, 9.

Bishnoi S., Rochelle G.T. (2002) Thermodynamics of piperazine/methyldiethanolamine/water/carbon dioxide, *Ind. Eng. Chem. Res.* **41**, 604–612.

Bosoaga A., Masek O., Oakey J.E. (2009) CO_2 capture technologies for cement industry, *Energy Procedia* **1**, 133–140.

Cadours R., Bouallou C. (1998) Rigorous simulation of gas absorption into aqueous solutions, *Ind. Eng. Chem. Res.* **37**, 1063–1070.

IEA Greenhouse gas R and D Programme. (2008) CO_2 capture in the cement industry, 2008/3, July 2008.

Intergovernmental Panel on Climate Change. (IPCC, 2013).

Kanniche M., Gros-Bonnivard R., Jaud Ph., Valle-Marcos J., Amann J.-M., Bouallou C. (2010) Precombustion, postcombustion and oxycombustion in thermal power plant for CO_2 capture, *Appl. Therm. Eng.* **30**, 53–62.

Knuutila H.K., Nannestad A. (2017) Effect of the concentration of MAPA on the heat of absorption of CO_2 and on the cyclic capacity in DEEA-MAPA blends, *Int. J. Greenh. Gas Control.* **61**, 94–103.

Lecomte F., Broutin P., Lebas E. (2009) Le captage du CO_2 des technologies pour réduire les Émissions de gaz à effet de serre, Édition technip, IFP publication.

Mehassouel A., Derriche R., Bouallou C. (2016) A new CO_2 absorption data for aqueous solutions of N-methyldiethanolamine + hexylamine, *Chem. Eng.Trans.* **52**, 595–600.

Mudhasakul S., Ku H.M., Douglas P.L. (2013) A simulation model of a CO_2 absorption process with methyldiethanolamine solvent and piperazine as an activator, *Int. J. Greenh. Gas Control.* **15**, 134–141.

Nazmul H.S.M. (2005) Techno-Economic study of CO_2 captures process for cement plants, Master thesis, University of Waterloo, Ontario, Canada.

Passalacqua R., Centi G., Perathoner S. (2015) Solar production of fuels from water and Co_2: Perspectives and opportunities for a sustainable use of renewable energy, *Oil Gas Sci. Technol. – Rev. IFP Energies nouvelles* **70**, 799–815.

Paul S., Ghoshal A.K., Mandal B. (2009) Kinetics of absorption of carbon dioxide into aqueous blends of 2-(1-piprazinyl)-ethylamine and N-methyldiethanolamine, *Chem. Eng. Sci.* **64**, 1618–1622.

Pinto D.D., Monteiro J.G.M.-S., Bersas A., Haug-Warberg T., Svendsen H.F. (2013) eNRTL parameter fitting procedure for blended amine systems: MDEA-PZ case study, *Energy Procedia* **37**, 1613–1620.

Raynal L., Alix P., Bouillon P.A., Gomez A., de Nailly M.F., Jacquin M., Kittel J., di Lella A., Mougin P., Trapy J. (2011a) The DMX^{TM} process: An original solution for lowering the cost of post-combustion carbon capture, *Energy Procedia* **4**, 779–786.

Raynal L., Bouillon P.A., Gomez A., Broutin P. (2011b) From MEA to demixing solvents and future steps, a roadmap for lowering the cost of post-combustion carbon capture, *Chem. Eng. J.* **171**, 742–752.

Sharifi A., Omidbakhsh Amiri E. (2017) Effect of the tower type on the gas sweetening process, *Oil Gas Sci. Technol. – Rev. IFP Energies nouvelles* **72**, 24.

Tan M. Sc. (2010) Study of CO_2 absorption into thermomorphic lipophilic amine solvents, Ph.D. Dissertation, University of Dortmund, Germany.

Toro-Molina C., Bouallou C. (2013) Kinetics study and simulation of CO_2 absorption into mixed aqueous solutions of methyldiethanolamine and diethanolamine, *Chem. Eng. Trans.* **35**, 319–324.

Tursunov O., Kustov L., Kustov A. (2017) A brief review of carbon dioxide hydrogenation to methanol over copper and iron based catalysts, *Oil Gas Sci.* Te*chnol. – Rev. IFP Energies nouvelles* **72**, 30.

Wang L., An S., Li Q., Yu S., Wu S. (2
017) Phase change behavior and kinetics of CO_2 absorption into DMBA/DEEA solution in a wetted-wall column, *Chem. Eng. J.* **314**, 681–687.

Whitman W.G. (1923) Preliminary confirmation of the two-film theory of gas absorption, *Chem. Met. Eng.* **29**, 146–148.

Xu Z., Wang S., Liu S., Chen C. (2012) Solvent with low critical solution temperature for CO_2 capture, *Energy Procedia* **23**, 64–71.

Xu Z., Shujuan W., Bo Z., Changhe C. (2013) Study on potential biphasic solvents: Absorption capacity, CO_2 loading and reaction rate, *Energy Procedia* **37**, 494–498.

Ye Q., Wang X., Lu Y. (2015) Screening and evaluation of novel biphasic solvents for energy-efficient post-combustion CO_2 capture, *Int. J. Greenh. Gas Control.* **39**, 205–214.

Ye Q., Zhu L., Wang X., Lu Y. (2017) On the mechanisms of CO_2 absorption and desorption with phase transitional solvents, *Int. J. Greenh. Gas Control.* **56**, 278–288.

Zhang J., Nwani O., Tan Y., Agar D.W. (2011) Carbon dioxide absorption into biphasic amine solvent with solvent loss reduction, *Chem. Eng. Res. Des.* **89**, 1190–1196.

Zhang J., Qiao Y., Agar D.W. (2012a) Improvement of lipophilic-amine-basedthermomorphic biphasic solvent for energy-efficient carbon capture, *Energy Procedia* **23**, 92–101.

Zhang J., Qiao Y., Agar D.W. (2012b) Intensification of low temperature thermomorphic biphasic amine solvent regeneration for CO_2 capture, *Chem. Eng. Res. Des.* **90**, 743–749.

Zhang J., Qiao Y., Wang W., Misch R., Hussain K., Agar D.W. (2013) Development of an energy efficient CO_2 capture process using thermomorphic biphasic solvents, *Energy Procedia* **37**, 1254–1261.

Zoghi A.T., Feyzi F., Zarrinpashneh S. (2012) Experimental investigation on the effect of addition of amine activators to aqueous solutions of N-methyldiethanolamine on the rate of carbon dioxide absorption, *Int. J. Greenh. Gas Control.* **7**, 12–19.

Appendix A

Physicochemical properties for the mixture MDEA–H_2O–CO_2

$$\left(H_{CO_2}\right)_{sol-MDEA} = \left(H_{N_2O}\right)_{sol-MDEA}\left(\frac{H_{CO_2}}{H_{N_2O}}\right)_{water}, \quad (A1)$$

$$\ln\left(H_{N_2O}\right)_{sol-MDEA} = HE_{water-MDEA} + x_{water}\ln\left(H_{N_2O}\right)_{water} + x_{MDEA}\ln\left(H_{N_2O}\right)_{MDEA}, \quad (A2)$$

$$HE_{water-MDEA} = x_{water}x_{MDEA}(23.378 - 0.0659T - 2.427x_{MDEA}), \quad (A3)$$

$$\left(H_{N_2O}\right)_{water} = 8.7407 \times 10^6\exp(-2284/T)\,(Pa{\cdot}m^3{\cdot}mol^{-1}), \quad (A4)$$

$$\left(H_{N_2O}\right)_{MDEA} = 1.524 \times 10^5\exp(-1312.7/T)\,(Pa{\cdot}m^3{\cdot}mol^{-1}), \quad (A5)$$

$$\left(H_{CO_2}\right)_{water} = 2.82 \times 10^6\exp\left(-\frac{2044}{T}\right)(Pa{\cdot}m^3{\cdot}mol^{-1}), \quad (A6)$$

CO_2 diffusivity

$$\left(D_{CO_2}\right)_{sol} = \left(D_{N_2O}\right)_{sol}{\cdot}\left(\frac{D_{CO_2}}{D_{N_2O}}\right)_{water}, \quad (A7)$$

$$\frac{\left(D_{N_2O}\right)_{water}}{\left(D_{N_2O}\right)_{sol}} = \left(\frac{\mu_{sol}}{\mu_{water}}\right)^{0.8}, \quad (A8)$$

$$\left(D_{N_2O}\right)_{water} = 5.07 \times 10^{-6}\exp\left(-\frac{2371}{T}\right), \quad (A9)$$

$$\left(D_{CO_2}\right)_{water} = 2.35 \times 10^{-6}\exp\left(-\frac{2119}{T}\right). \quad (A10)$$

MDEA diffusivity

$$\left(D_{MDEA}\right)_{sol} = \left(D_{CO_2}\right)_{sol}{\cdot}\left(\frac{D_{CO_2}}{D_{MDEA}}\right)_{water}{\cdot}\left(\frac{\mu_{water}}{\mu_{sol}}\right)^{0.2}, \quad (A11)$$

$$\left(D_{MDEA}\right)_{sol} = \frac{\left(D_{CO_2}\right)_{sol}}{2.43}\left(\frac{\mu_{water}}{\mu_{sol}}\right)^{0.2}. \quad (A12)$$

Appendix B

Appendix B. Results of the validity tests of the correlation used for the estimation of the liquid side mass transfer coefficient (*kl*).

Solvent (wt.%)	Re	Sc	Sh
MDEA 40 wt%			
298 K	644.43	9972.29	966.91
MDEA 37 wt.% + HA 3 wt.% 298 K			
313 K	608.004	11008	971.25
333 K	1016.53	3778.93	882
	1743.24	1170.64	769.03
MDEA 35 wt.% + HA 5 wt.%			
298 K	630.03	10268.30	963.9
313 K	1036.44	3626.79	869.49
333 K	1741.33	1166.47	769.03
MDEA 33 wt.% + HA 7 wt.%			
298 K	601.81	11122.01	971.73
313 K	1199.54	3889.27	981.92
333 K	1745.23	1160.37	768.08